PCCP

Accepted Manuscript

ROYAL SOCIETY OF CHEMISTRY

www.rsc.org/pccp

Cite this: DOI: 10.1039/c0xx00000x

www.rsc.org/xxxxxx

ARTICLE TYPE

Electronic structure and spectra of $(Cu_2O)n$-H_2O complexes

Ioannis D. Petsalakis,*[a,b] Giannoula Theodorakopoulos[a,b] and Jerry Whitten[b]

Received (in XXX, XXX) Xth XXXXXXXXX 20XX, Accepted Xth XXXXXXXXX 20XX
DOI: 10.1039/b000000x

Density Functional Theory calculations have been employed to determine optimized geometries for different $(Cu_2O)_n$ clusters for n=1 to 6, 12 and 18. The results show formation of $(Cu_2O)_n$ rings for n≥2, while $(Cu_2O)_n$ nanobarrels have been determined for n= 12 and for n=18. Adsorption of H_2O on the $(Cu_2O)_n$ clusters occurs preferentially by interaction of the water O with outer Cu atoms. Calculated absorption spectra by Time Dependent Density Functional Theory show that in all cases charge-transfer excitations from occupied orbitals of the $(Cu_2O)_n$ cluster to a Rydberg orbital of H_2O, contribute to the character of the singlet excited states calculated at energies starting at about 2.6 eV, with increasing contribution found at higher excitation energies. Configuration interaction calculations on selected $(Cu_2O)_n$-H_2O complexes determine charge-transfer excitations to contribute significantly to excited states lying at 4.6-6.2 eV above the ground state.

Introduction

Cuprous oxide (Cu_2O), is a p-type semiconductor, with a high optical absorption coefficient and a bulk band gap of 2.2 eV and it is considered to be an excellent candidate for applications in solar energy photovoltaics and photocatalysis.[1-5] The question of Cu_2O acting as a photocatalyst for water splitting under visible light irradiation is still open and of particular experimental interest.[4,5,6] Theoretical investigations employing DFT-based and periodic slab methods have been devoted to the investigation of the adsorption and dissociation of H_2O on Cu_2O surfaces[7], reporting that Cu_2O is a promising photocatalyst for water splitting, while ground-state dissociative adsorption of H_2O on Cu_2O(110):CuO surface appears to be only slightly endothermic.[8] Similarly, the bonding of H_2X (for X=O, S) on cluster models of CuO(111) has been investigated by DFT calculations.[9]

Metal oxide nanoparticles have been widely studied as they form an intermediate between the molecular and the bulk state and accordingly may have different properties depending on their size and symmetry.[1,2] The possibility of rationally tuning the optical properties of Cu_2O through the control over the dimensions and morphologies of Cu_2O nanostructures, has stimulated a large number of efforts devoted to the fabrication of a range of Cu_2O nanostructures,[1,2] including nanocubes,[3] nanospheres[10] and nanorings.[11] However, only a few applications of nanoscale Cu_2O to water photoelectrochemistry are known.[12]

The formation of $(Cu_2O)_n$ clusters has been investigated by DFT calculations on neutral and cationic, hydrated and hydrogenated clusters for n=1 and 2[13], while DFT and TDDFT calculations have been performed on n=1,2 and 3 clusters[2] and also on Cu_2O_m (m=1,4) clusters.[14] Thus for $(Cu_2O)_n$ clusters DFT calculations have been reported only for n up to 3 whereas for CuO larger clusters, including nanotube-analogues with a square unit mesh rather than the hexagonal mesh of carbon nanotubes, have been calculated by DFT.[15] It is thus of interest to determine the structure of larger than n=3 $(Cu_2O)_n$ clusters and possible stable structures for cuprous oxide nanotubes or nanobarrels.

In the present work the formation of different Cu_2O clusters, including nanorings and nanobarrels has been investigated, as well as the adsorption of H_2O on these clusters, by theoretical calculations in an effort to determine their electronic structure and spectra. In this manner, fundamental information of relevance to different applications is determined including the interesting question of the photocatalysis of H_2O splitting by Cu_2O.

Calculations and results

DFT[16] and TDDFT[17] calculations have been carried out on different $(Cu_2O)_n$ clusters for n=1 to 6, 12 and 18 and $(Cu_2O)_n$-H_2O complexes for n=1 to 6. The optimum geometries for all clusters and complexes have been determined using the

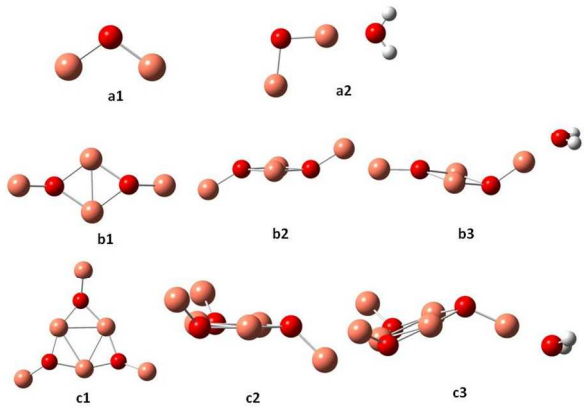

Fig.1 Optimized ground state geometries for $(Cu_2O)_n$ and $(Cu_2O)_n$-OH_2, for n=1, 2 and 3. Small red spheres O, large faded red spheres Cu and small white spheres H atoms.

Cite this: DOI: 10.1039/c0xx00000x

www.rsc.org/xxxxxx

ARTICLE TYPE

Table I. Geometrical parameters[a] of the optimum $(Cu_2O)_n$ structures for n=1-6, Cu-OH_2 distance and binding energy of H_2O on the clusters

n	Cu-O (ring) Å	Cu-O outer Å	<CuOCu ring °	<OCuO ring °	Dih. Angles Outer Cu °	Cu-OH_2 Å	BE eV
1	1.757	-	108.7			1.904	0.96
2	1.909	1.763	70.5	109.5	133.5	1.900	1.06
3	1.843 ± 0.003	1.765 ± 0.001	83.3 ± 0.3	156.2 ± 0.6	119.6 ± 2.3	1.895	1.09
4	1.812 ± 0.003	1.7658	99.1 ± 0.1	171.0 ± 0.3	128.1 ± 1.6	1.895	1.11
5	1.801 ± 0.002	1.773 ± 0.001	111.3 ± 1.5	175.5 ± 1.5	131.4 ± 2.3	1.896	1.09
6	1.797 ± 0.002	1.775 ± 0.001	119.0 ± 0.8	179.6 ± 0.3	133.2 ± 1.2	1.897	1.10
6[b]	1.855 ± 0.002	1.836 ± 0.002	117.8 ± 1.0	177.8 ± 0.5	119.2 ±1.2	-	-

[a] average values [b]calculated with B3LYP/LANL2D

B3LYP[18] functional and LANL2DZ basis set[19] and, in addition, for the smaller clusters, i.e. for n=1 to 6, with the aid of B3LYP and 6-311G(d,p) basis set. It is not practical to employ the 6-311G(d,p) basis set for the n=12 and n=18 clusters as the geometry optimization calculations become extremely time consuming. The excited states of the n=1 to 6 clusters as well as those of their corresponding complexes with H_2O, at the ground state geometries, have been calculated by TDDFT employing the M062X[20] functional and 6-311+G(d,p) basis set, i.e. including diffuse functions, provided in Gaussian 09.[21] Since charge-transfer type of states, i.e. those involving excitations from $(Cu_2O)_n$ to H_2O, it is not appropriate to employ the B3LYP functional as it would result in underestimation of the excitation energies. For the n=12 and n=18 clusters TDDFT calculations employing the 6-311+G(d,p) basis set become too large and not practical. For this reason, configuration interaction calculations have been employed for the excited states of structures involving adsorption of H_2O on n=18, n=12 clusters, which pose difficulties to TDDFT and also for H_2O on the n=4 cluster for comparison with TDDFT. Details of the CI calculations will be provided in section B cf. below and in the ESI.

A. Geometries of $(Cu_2O)_n$ and $(Cu_2O)_n$-H_2O, n=1-6

The coordinates for all the optimum structures determined in the present work are available in the Electronic Supplementary Information (ESI). In Figure 1, the optimized geometries for $(Cu_2O)_n$ and $(Cu_2O)_n$-OH_2 clusters for n=1,2 and 3 are shown and in Figure 2 the corresponding structures for n=4-6. In Table I the geometrical parameters for the optimized structures for all clusters, n=1-6 are listed, where average values of the bond lengths and angles are given when there are differences. Further details on the geometries may be generated from the data in the ESI. In the triatomic Cu_2O (cf. a1 in Fig.1) the Cu-O bond lengths are calculated as 1.757 Å and the angle <CuOCu as 108.7˚. A water molecule is attached to Cu_2O, with binding energy of 0.96 eV, by interaction of the oxygen atom of water with one of the Cu atoms, with the Cu-OH_2 distance 1.904 Å cf. a2 in Fig.1 and Table I. Attachment of H_2O leads to slight elongation of the closer O-Cu bond to 1.765 Å, a very slight shortening of the other Cu-O bond to 1.752 Å and a slight opening of the bond angle to 109.1˚. The n=2 cluster, cf. b1 and b2 in Fig.1, shows the formation of a four-membered ring and two non-ring Cu atoms above and below the plane of the ring, at a dihedral angle of 133.5˚. Accordingly different bond lengths are calculated for O-Cu in the ring, at 1.909 Å, and the O-Cu non-ring 1.763 Å. The bond angles are different as well, with the <CuOCu within the ring at 70.5˚ and the outer angle at 134.3˚. In the ring, the <OCuO angles are calculated at 109.5˚. As found for n=1, a water molecule is attached to the n=2 cluster, cf. b3, by interaction of the water oxygen with one of the non-ring Cu atoms at a distance of 1.900 Å and a binding energy of 1.06 eV. Similar to n=2, the n=3 cluster also favours the formation of a ring, this time 6-membered as shown in c1, with large <OCuO ring angles (156.2±0.6˚) cf Fig. 1 and Table I. It may also be noted that generally the ring Cu-O bond lengths are larger than the outer Cu-O bond lengths, as noted for the n=2 cluster. Again in the lowest energy structure, H_2O attaches by interaction with one of the outer Cu atoms at a Cu-O distance of 1.895 Å and binding energy of 1.09 eV. As was the case for n=1, attachment of H_2O causes small distortions of the bond lengths and angles of the optimum structures of the clusters, and detailed structures

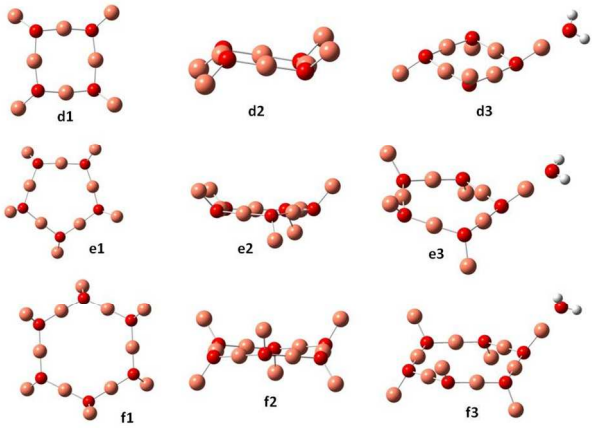

Fig.2 Optimized ground state geometries for $(Cu_2O)_n$ and $(Cu_2O)_n$-OH_2, for n=4, 5 and 6. Small red spheres O, large faded red spheres Cu and small white spheres H atoms.

Cite this: DOI: 10.1039/c0xx00000x

www.rsc.org/xxxxxx

ARTICLE TYPE

may be generated from the ESI data. There is good agreement between the present (cf. Figure 1) and the previously reported structures for a1,[2, 13, 22] a2, b1 and b3 of the present work.[13]

Previously reported geometries for $(Cu_2O)_n$ with n=2 and 3[2] are found to be higher in energy than the optimum structures b2 and c2 of Fig. 1, where however the cis analogues of b2 and c2, ie., with all singly coordinated Cu atoms in the same direction with respect to the plane of the ring[2] are only slightly higher in energy, by 0.03 and 0.1 eV respectively. Geometry optimization of the larger clusters, i.e. for n=4 , 5 and 6, resulted in the structures shown in Figure 2. As shown, as a rule, rings are formed, where the sides are made up by nearly linear O-Cu-O segments (179˚), with another Cu atom at each O atom out of the plane of the ring, cf. also structures b and c for n=2 and 3 of Figure 1. The ring Cu-O bond lengths are around 1.800-1.810 Å, with the outer at 1.770-1.776Å. In the cuprite bulk unit cell of Cu_2O, the oxygen atom is surrounded by four Cu atoms, while each Cu atom is coordinated with two O atoms,[23] with Cu-O distance of 1.849 Å. The present results show that in the ring structures of Figures 1 and 2, O is coordinated with three Cu atoms, ring Cu atoms are coordinated with two O atoms and outer Cu atoms with one O atom. These latter Cu atoms offer the preferable position of attachment of H_2O, via interaction with the water oxygen, in all the n=1-6 clusters calculated in the present work. The resulting structures are given as a2, b3 and c3 in Figure 1 and d3, e3 and f3 in Figure 2. The angle O-Cu-OH_2 is at 179˚ in all cases and the Cu-OH_2 distance at about 1.90Å (cf. Table I). These structures are the lowest energy structures obtained by optimization calculations, while other types of attachment, eg. by hydrogen bonding lead to higher energy structures. The binding energy of adsorbed H_2O is around 1 eV for all clusters calculated.

Comparison with the results of B3LYP/LAN2DZ calculations on the n=1-6 clusters shows that the same basic structure is obtained in each case but with some elongation of the bonds. An example of the results obtained by B3LYP/LAN2DZ is given in the last row of Table I for n=6, showing the differences in the geometrical parameters obtained as compared to those obtained with the 6-311G(d,p) basis set.

B. Cu_2O nanobarrels

As noted in the Introduction, different types of nanoclusters of Cu_2O have been synthesized[1,2] and studied by classical electrodymanics.[2] Here different tubes of $(Cu_2O)_n$ are constructed, and they are shown in Fig.3. Nanobarrels 1a and 1b of Fig.3, with n=18 and 12 respectively, have been constructed using the coordination of Cu and O in bulk Cu_2O and adsorption of one H_2O on these clusters. Determination of the excited states of the n=18 and 12 clusters and those of their complexes with H_2O by TDDFT became very cumbersome because with increasing n the number of low-lying electronic states rapidly increases. Furthermore the calculations on the smaller systems indicated the necessity for diffuse functions in the basis set, making proper TDDFT treatment of the n=18 and 12 clusters and complexes not practical. Thus for these larger complexes a configuration interaction (CI) method of calculation was employed for the excited charge-transfer states. The CI method employed has been described in previous work on a $(Ti_6O_{12})_3$ nanotube[24] and elsewhere.[25] Further details of the CI method and calculations are given in the ESI. Geometry optimization calculations of structures 1c,1d, 2a and 2c of Fig.3 have been carried out by DFT/B3LYP/LAN2LDZ calculations as the clusters are too large for the 6-311G(d,p) basis set. In structures 1a and 1b only the position of H_2O has been optimized, with the Cu_2O cluster geometry kept frozen in the CI calculations. Structures 1c and 1d

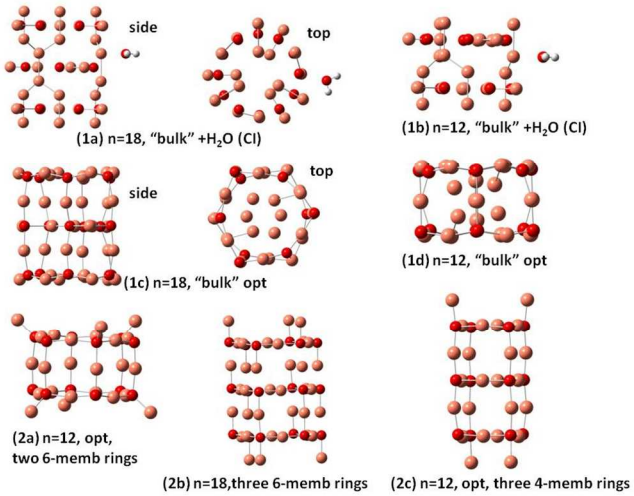

Fig.3 Optimized structures of nanobarrels. Small red spheres O and large faded red spheres Cu atoms.

result from optimization of the n=18 1a and n=12 1b clusters, respectively. Nanobarrels 2a, 2b and 2c have been constructed by stacking d1 and f1 rings (of Fig.2) and subsequent geometry optimization. Structure 2a is made up by stacking two n=6 rings, 2b by stacking three n=6 rings and 2c by stacking three 4-membered rings. Geometry optimization was nearly but not fully

Table II Excitation Energy to the lowest singlet excited state of the $(Cu_2O)_n$-H_2O complexes and the lowest singlet state with Rydberg H_2O character

n	S_1 ΔE (eV), f-value	S_{Ryd} root no, ΔE (eV), f-value	H_2O Rydberg orbital
1	2.01, 0.001/2.00,[a] 0.015[a]	(1), 2.01, 0.001	LUMO+1
2	2.02, 0.006/1.92,[a] 0.063[a]	(4), 2.65, 0.003	LUMO+1
3	2.07, 0.005/2.14,[a] 0.003[a]	(7), 3.08, 0.011	LUMO+2
4	2.07, 0.005/2.12,[a] 0.002[a]	(12), 3.07, 0.010	LUMO+3
5	2.07, 0.001/2.11,[a] 0.002[a]	(15), 3.11, 0.014	LUMO+4
6	2.08, 0.001/2.14,[a] 0.000[a]	(16), 3.10, 0.015	LUMO+5

[a] corresponding values for $(Cu_2O)_n$.

Cite this: DOI: 10.1039/c0xx00000x

www.rsc.org/xxxxxx

ARTICLE TYPE

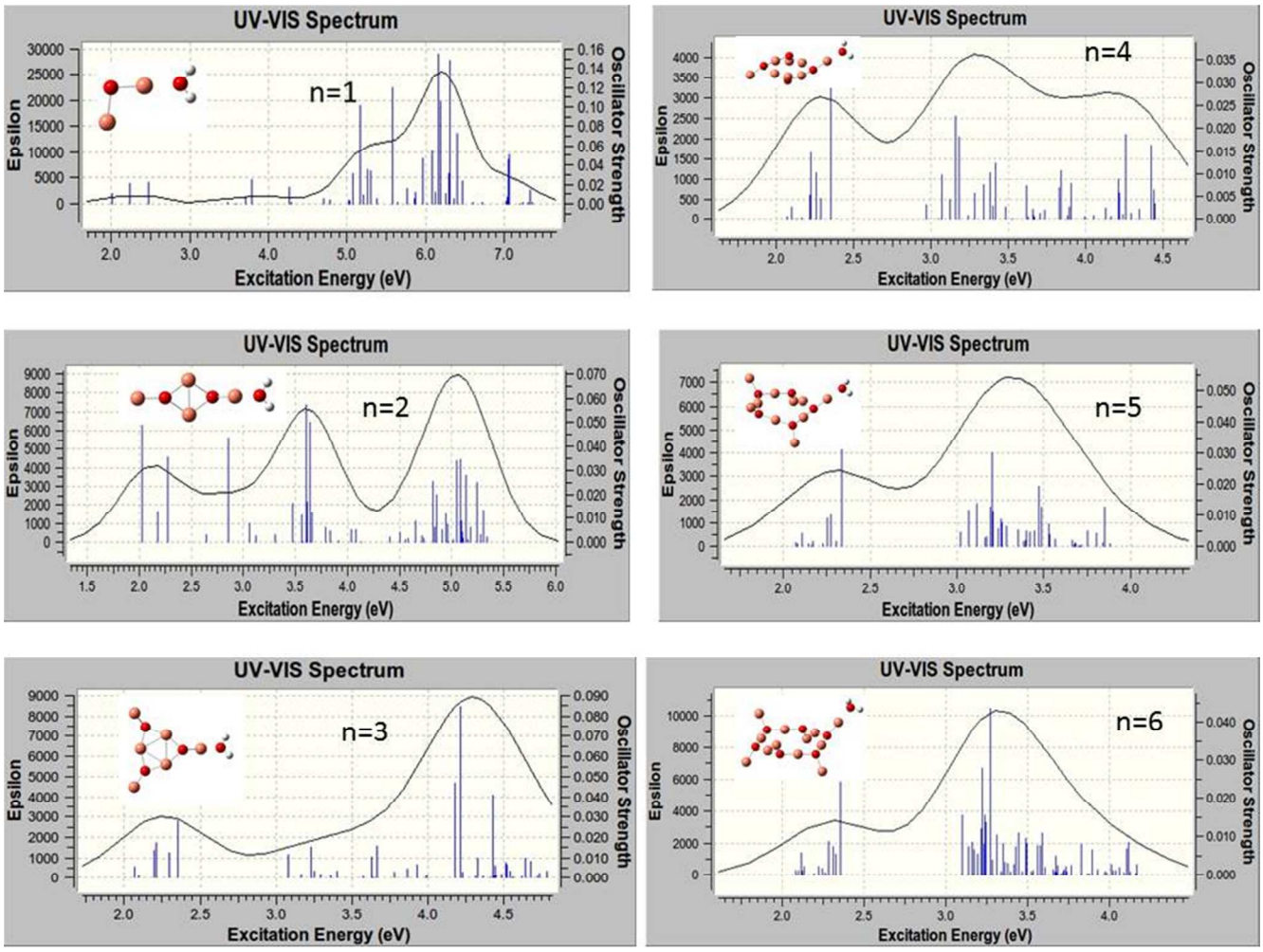

Fig.4 Calculated absorption spectra of $(Cu_2O)_n$-OH_2

converged for the n=18 structure 2b, of figure 3 as the calculation was oscillating between slightly different structures. The results show that in the optimized structures 2a and 2c but also in 2b square surface units are formed, of side O-Cu-O and length at 3.8 Å, resembling the square ring of the n=4 cluster, cf. d1 of Fig. 2. It should be noted that the optimized structures 1c and 1d of Fig. 3, also have the square surface unit, even though the starting geometries for the optimization are quite different. Square surface units have been also reported for CuO nanotubes,[15] whereas in carbon nanotubes the surface units are hexagons. Optimized structures (1d) and (2a) are similar with their main difference being that the outwards pointing Cu atoms in (2a) are pointing inward in (1d). Of the n=12 structures, (2c) has the lowest energy with structure, (1d) lies higher only by 0.32 eV but (2a) lies at 3.1 eV above 2c. All clusters $(Cu_2O)_n$ are bound with respect to dissociation to Cu_2O units, with each added Cu_2O unit to a $(Cu_2O)_{n-1}$ cluster increasing the binding by 2.5-3.6 eV, depending on n. These results show that it is possible to form stable geometries resembling nanotubes, in agreement with experimental reports of the formation of Cu_2O nanoclusters of different shape. The different nanoclusters are bound with respect to dissociation and the relative stability will depend on the size of the clusters.

The present calculations on the structure of two types of clusters namely the n=1-6 $(Cu_2O)_n$ clusters and the n=12 and n=18 clusters show that formation of such clusters is favorable and the two types are related in the sense that the stacking of the rings determined for the n=1-6 $(Cu_2O)_n$ clusters lead to stable nanotube or nanobarrels structures, as has been found for structures 2a and ab of Fig. 3 involving stacking of n=6 units and for structure 2c of Fig.3 involving stacking of n=4 units.

C. Excited states and absorption spectra

The excited electronic states of the clusters $(Cu_2O)_n$ and the

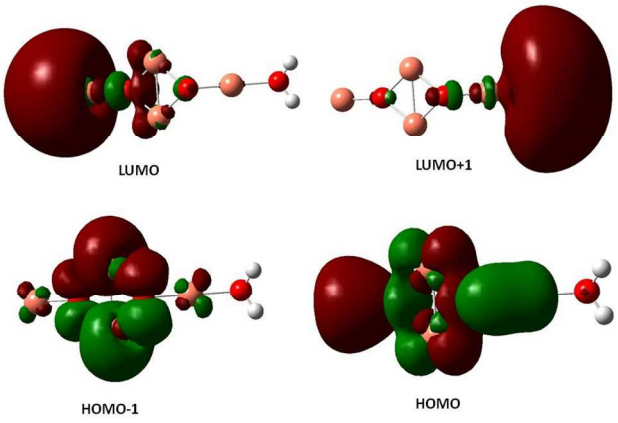

Fig.5. Electron density plots of the two highest occupied and the two lowest unoccupied orbitals of the $(Cu_2O)_2$-OH_2complex

complexes $(Cu_2O)_n$-OH_2 for n=1-6 have been calculated by TDDFT/M062X/6-311+G(d,p), for 80-100 roots. The resulting absorption spectra of the $(Cu_2O)_n$ clusters alone are given Figure S1 in the ESI while spectra of the complexes with water in Figure 4. The lowest singlet excited state of all the clusters lies at excitation energy of about 2.0 eV with very low oscillator strengths cf. Table II. Adsorption of H_2O does not alter the appearance of the absorption spectra, cf. Figs 4 and S1. However on closer examination of the excited states it is shown that in the $(Cu_2O)_n$-OH_2 systems, excitations into an unoccupied Rydberg orbital of H_2O contribute to the excited states for all n calculated. For example, for the case of n=1, the second lowest unoccupied orbital (or LUMO+1) is a Rydberg orbital of H_2O, and even the first excited state at 2.01 eV has a contribution from a charge-transfer excitation, i.e. excitation from an occupied Cu_2O orbital to the H_2O unoccupied Rydberg orbital, with a coefficient 0.2. For higher excited states, the charge-transfer contribution increases, eg. its coefficient becomes 0.81 for an excited state Cu_2O-OH_2 at 3.48 eV. Similarly, for the higher n clusters, the Rydberg orbital of H_2O is one of the lower unoccupied orbitals, cf. Table II, and charge transfer excitations contribute to the character of the excited states of the complexes starting at the excited state indicated in Table II. Electron density plots of the two highest occupied and two lowest unoccupied orbitals for the n=2 complex (cf. b3 in Fig.1) are plotted in Figure 5, where it can be seen that LUMO+1 is a Rydberg orbital belonging to H_2O. This is characteristic of the type of MO electron density plots of all the complexes, for the particular virtual orbital in each case.

It might be noted that in the absorption spectra of the larger complexes, i.e., for for n≥3, cf. Fig.4, the lowest excited state in which there is H_2O contribution occurs around 3.1 eV, cf. Table II, with a group of cluster excited states between about 2.0 and 2.4 eV followed by a gap, without any states until 3.0-3.1 eV. In addition, for these complexes the density of states becomes increasing high and excitation energies over 4.5-5.0 eV are not reached for the calculated roots, which are 80-100, depending on the system.

The lowest excited state of the free H_2O molecule is at vertical excited energy at 7.4 eV from the ground state and although it has Rydberg character at the vertical point, it is in fact dissociating to yield OH+H.[26] The possibility of populating a virtual orbital of H_2O adsorbed on $(Cu_2O)_n$ at lower energy than the free water absorption might be of interest for the question of photocatalytic splitting of H_2O at clusters of Cu_2O. However, geometry optimization of the lowest excited state of Cu_2O-H_2O, carried out here, resulted in a stable geometry (i.e. not dissociating) for the S_1 state of Cu_2O-OH_2, with emission spectrum only slightly red shifted with respect to the absorption spectrum. Geometry optimization of higher-lying excited states, with heavier contribution of the charge-transfer excitation is technically not possible as the density of states is high and there exist many nonadiabatic interactions. The charge-transfer contribution for the higher n complexes starts at higher-lying states, cf. Table II. Finally, the charge-transfer states of the n=18 and n=12 complexes with water, cf. structures 1a and 1b of Figure 3, and also for the n=4 cluster, d1 of Fig. 2, have been determined with CI calculations. The CI results show that charge transfer excitations have small contributions to low-lying states while the more significant contributions (coefficients 0.4-0.6) are found for higher lying excited states, for n=4 at excitation energies from 4.77 – 4.91 eV, for n=12 at excitation energies from 4.57-6.14 eV and for n=18 from 4.52-5.11 eV (cf. ESI).

The results of the calculations on the excited states, both TDDFT and CI, show that adsorption of a single water molecule on Cu_2O clusters induced charge-transfer type excitations contributing to the electronic excited states, at energies well below the lowest singlet excitation energy of free H_2O.

Conclusions

Geometry optimization DFT/B3LYP/6-311G(d,p) calculations have been carried out on $(Cu_2O)_n$ clusters and $(Cu_2O)_n$-OH_2 complexes for n=1-6 and DFT/B3LYP/LAN2LDZ calculations on $(Cu_2O)_n$ clusters with n=12 and 18. Minimum energy structures have been determined, all bound with respect to dissociation to Cu_2O substituent units. The results for n=2-6 show the formation of rings enabling coordination of the O atoms with three Cu atoms, of which one is coordinated to one O atom and lies above or below the ring. The ring Cu atoms are coordinated to two O atoms in a nearly linear arrangement, when the dimensions of the cluster allow it. Trans arrangements of the non-ring cu atoms is slightly more favourable to cis. In all cases, adsorption of one molecule of H_2O occurs by interaction between the water O and one of the non-ring Cu atoms, with binding energies of about 1.0 eV. Suggestions are made for the formation of $(Cu_2O)_n$ nanobarrels for n=12 and 18 and different structures have been determined, showing a square mesh surface structure.

Configuration interaction calculations have been carried out on adsorbed H_2O on n=18 and n=12 nanobarels.

The excited states of $(Cu_2O)_n$ clusters and $(Cu_2O)_n$-OH_2 complexes for n=1,6 have been calculated by TDDFT/M062X/6-311+G(d,p) calculations at their optimum ground state geometry and for n=1 at the optimum geometry of the S_1 state as well. The results show that the lowest electronic state of these systems lies at excitation energy from the ground state of about 1.92-2.14 eV and the low energy absorption spectra have generally low oscillator strengths. In all complexes, a Rydberg-type H_2O virtual orbital contributes to the character of the excited states, starting at the first excited state (at 2.01 eV) for n=1, at the fourth excited state (2.65 eV) for n=2 and at higher excited states (at 3.07-3.11 eV) for the larger complexes. The contribution of charge-transfer excitations becomes significant for higher lying excited states, calculated by CI at excitation energies of 4.5 – 6.14 eV, for different complexes. The present calculations are consistent with a possible photocatalytic function of Cu_2O for water splitting.

Notes and references

[a] *Theoretical and Physical Chemistry Institute, The National Hellenic Research Foundation, 48 Vassileos Constantinou Ave, Athens 116 35,Greece. Fax: +30210 7273794; Tel: +30210 7273807; E-mail: idpet@eie.gr*

[b] *Department of Chemistry, North Carolina State University, Raleigh, North Carolina, 27695, USA, Fax: (919) 515-5079;Tel: (919) 515-7960; E-mail:whitten@ncsu.edu*

† Electronic Supplementary Information (ESI) available: [details of any supplementary information available should be included here]. See DOI: 10.1039/b000000x/

1 L. Zhang and H. Wang, *ACS NANO*, 2011, **5**, 3257.
2. B. Sinha, T. Goswami, S. Paul and A. Misra, *RSC Adv.*, 2014, **4**, 5092.
3. M. Zahmakıran, S. Özkar, T. Kodaira and T. Shiomi, *Materials Letters*, 2009, **63**, 400.
4. M. Hara, T. Kondo, M. Komoda, S. Ikeda, K. Shinohara, A. Tanaka, J. N. Kondo and K. Domen, *Chem. Commun.,* 1998, 357.
5. P. E. de Jongh, D. Vanmaekelbergh and J. J. Kelly, *Chem. Commun.,* 1999, 1069.
6. P. H. Reddy, H. Sekhar and D. N. Rao, *PRAMANA- J. Phys.*, 2014, **82**, 321.
7. L. I. Bendavid and E. A. Carter, *J. Phys. Chem. B,* 2013, **117**, 15750.
8. S. A. Saraireh and M. Altarawneh, *Can. J. Phys.*, 2013, *91*, 1101.
9. M. Casarina, C. Maccato, N. Vigato and A. Vittadini, *Applied Surface Science*, 1999, **142**, 164.
10. J. Zhang, J. Liu, Q. Peng, X. Wang, and Y. Li, *Chem. Mater.*, 2006, **18**, 867.
11. R. K. Swarnkar and R. Gopal, *Sci. Adv. Mater.*, 2012, **4**, 511.
12. F. E. Osterloh, *Chem. Soc. Rev.*, 2013, **42**, 2294.
13. M. Jadraque and M. Martín, *Chem. Phys. Letters*, 2008, **456**, 51.
14. B. Dai, L. Tian and J. Yang, *J. Chem. Phys.*, 2004, **120**, 2746.
15. H. F. Farrell and R. D. Parra, *J. Vac. Sci. Technol. B*, 2011, **29**, 061806-1.
16. R.G. Parr, W. Yang *Annu. Rev. Phys. Chem.* 1995, **46**, 701.
17. M.A.L. Marques, E.K.U. Gross, *Annu. Rev. Phys. Chem.* 2004, **55**, 427.
18. A. D. Becke, *Phys. Rev. A* 1988, **38**, 3098
19. P. J. Hay, W.R. Wadt, *J. Chem.Phys.* 1985, **82**, 270; 284; 299.
20. Y. Zhao and D. Truhlar, *Theor. Chem. Acc.* 2008, **120**, 215; Y. Zhao and D. Truhlar, *Acc. Chem. Res.* 2008, **41**, 157.
21. Gaussian 09, Revision A.1, M. J. Frisch, G. W. Trucks, H. B. Schlegel, G. E. Scuseria, M. A. Robb, J. R. Cheeseman, G. Scalmani, V. Barone, B. Mennucci, G. A. Petersson, H. Nakatsuji, M. Caricato, X. Li, H. P. Hratchian, A. F. Izmaylov, J. Bloino, G. Zheng, J. L. Sonnenberg, M. Hada, M. Ehara, K. Toyota, R. Fukuda, J. Hasegawa, M. Ishida, T. Nakajima, Y. Honda, O. Kitao, H. Nakai, T. Vreven, J. A. Montgomery, Jr., J. E. Peralta, F. Ogliaro, M. Bearpark, J. J. Heyd, E. Brothers, K. N. Kudin, V. N. Staroverov, R. Kobayashi, J. Normand, K. Raghavachari, A. Rendell, J. C. Burant, S. S. Iyengar, J. Tomasi, M. Cossi, N. Rega, J. M. Millam, M. Klene, J. E. Knox, J. B. Cross, V. Bakken, C. Adamo, J. Jaramillo, R. Gomperts, R. E. Stratmann, O. Yazyev, A. J. Austin, R. Cammi, C. Pomelli, J. W. Ochterski, R. L. Martin, K. Morokuma, V. G. Zakrzewski, G. A. Voth, P. Salvador, J. J. Dannenberg, S. Dapprich, A. D. Daniels, O. Farkas, J. B. Foresman, J. V. Ortiz, J. Cioslowski, and D. J. Fox, Gaussian, Inc., Wallingford CT (2009).
22. D. A. Dixon and J. L. Gole, *Chem. Phys. Letters*, 1992, **189**, 390.
23. A. Soon, M. Todorova, B. Delley, and C. Stampfl, *Phys. Rev. B.*, 2007, **75**, 125420; 2007, **76**, 129902(E).
24. B. N. Papas and J. L. Whitten, J. Chem. Phys., 2013, **138**, 054312.
25. L. S. Sremaniak and J. L. Whitten, Surf. Sci., 2002, **516**, 254;2007, **601**, 3755; 2008, **602**, 834.
26. G. Theodorakopoulos, I. D. Petsalakis and R. J. Buenker, *Chem. Phys.*, 1985, **96**, 217; G. Theodorakopoulos, I. D. Petsalakis and R. J. Buenker, *Chem. Phys. Letters*, 1987, **138**, 71.